The Astrophysical Journal, 700:L51–L55, 2009 July 20 doi:10.1088/0004-637X/700/1/L51

GRADUAL SOLAR ENERGETIC PARTICLE EVENT ASSOCIATED WITH A DECELERATING SHOCK WAVE

L. Kocharov[1], T. Laitinen[1], A. Al-Sawad[1], O. Saloniemi[1], E. Valtonen[1], and M. J. Reiner[2,3]
[1] Space Research Laboratory, Department of Physics and Astronomy, University of Turku, Turku 20014, Finland
[2] The Catholic University of America, Washington, DC, USA
[3] NASA Goddard Space Flight Center, Greenbelt, MD 20771, USA
Received 2009 April 27; accepted 2009 June 18; published 2009 July 2

ABSTRACT

On 2000 April 4–6 the Energetic and Relativistic Nuclei and Electron particle telescope on the *Solar and Heliospheric Observatory* spacecraft observed a major solar energetic particle (SEP) event associated with two coronal mass ejections (CMEs) separated by approximately 8 hr. The first CME was accompanied by a low-frequency type II radio burst observed by the WAVES receivers on the *Wind* spacecraft. Analysis of the high-precision measurements of the ∼20 MeV proton flux anisotropy, model fitting of the type II dynamic spectrum, and SEP transport modeling support the idea that the shock wave of the first CME was an efficient accelerator for ∼20 MeV protons during only the first 6 hr after the launch. This shock gradually slowed down, weakened, and became transparent for the protons produced by the second eruption behind the previous CME. The main production of SEPs due to the two successive eruptions continued together for 12 hr. The near-Earth SEP event was additionally amplified by the SEP mirroring in the interplanetary magnetic field draping at the edge of an old CME beyond the Earth's orbit, which made the SEP intensity–time profiles more prolonged than would be expected based on the assumption of SEP transport in the standard solar wind.

Key words: acceleration of particles – shock waves – Sun: particle emission

1. INTRODUCTION

The widely accepted impulsive-gradual paradigm for solar energetic particle (SEP) events is an empirical classification system developed step-by-step by combining the SEP data, the X-ray and radio observations, and more recently the observations of coronal mass ejections (CMEs), and in its refined formulation suggests that in major, or gradual, SEP events the high-energy particles are produced at CME-driven shock waves in the solar wind, while impulsive SEP events originate from solar flares (e.g., Reames 1999). Recently, Marqué et al. (2006) analyzed CMEs with no radio signature of electron acceleration in the solar corona and found them not to be associated with the production of SEPs, while Cliver et al. (2004) and Gopalswamy et al. (2005) found that the majority of the metric-to-kilometric type II bursts were associated with SEP events. Those and a number of other observations support the idea that the production of SEPs in major events starts in the solar corona in association with the flare and CME liftoff and continues at interplanetary shocks.

If high-energy particles were continuously accelerated from the ambient material at the shock wave propagating at constant speed to 1 AU, one could expect that the most hazardous radiation intensities would occur only upon the shock arrival at the spacecraft, while in many major events the peak intensities of the high-energy protons are observed when the shock is still closer to the Sun than to the Earth (e.g., Neal et al. 2008). One of the factors shaping the intensity temporal profiles in gradual SEP events could be deceleration of associated shocks during their interplanetary propagation, and there have been a number of arguments in favor of decelerating shocks (Reiner et al. 2007, and references therein). However, SEP acceleration at such shocks has not yet received due attention.

For the history of a SEP production to be deduced, the SEP flux anisotropy data must be analyzed. That was not always done for gradual SEP events. We use high-precision 17–22 MeV proton flux anisotropy data from the Energetic and Relativistic Nuclei and Electron (ERNE) instrument on the *Solar and Heliospheric Observatory* (*SOHO*) spacecraft (Torsti et al. 1995). The high-energy detector (HED) of the ERNE instrument is capable of measuring the particle arrival directions with a high accuracy within its fixed viewcone of 120° × 120° (e.g., Torsti et al. 2004), while the interplanetary magnetic field direction varies, typically being within or slightly beyond the HED viewcone. Using the instrument's 241 directional bins, we define the proton pitch-angle distribution over the varying range of observable pitch angles. The SEP intensity and anisotropy profiles will be compared with the low-frequency type II radio emissions, which are generated by the CME-driven shocks, that are observed by the WAVES receivers on the *Wind* spacecraft (Bougeret et al. 1995).

We report here on the observations of the 2000 April 4–6 event, which is among the major SEP events of solar cycle 23 (Table 1 of Gopalswamy 2003). A distinctive feature of this event is that it was associated with more than one successive CME, and SEPs from a later CME can probe the earlier CME–shock complex in the interplanetary space. After reporting the observational results, we will use an SEP modeling for the data interpretation.

2. DATA ANALYSIS

On 2000 April 4, *SOHO*/ERNE detected an SEP event onset at 15:50–17:06 UT for proton energies 3.3–67 MeV, while *GOES* observed a gradual X-ray flare of class C9.7/2F, which started at 15:12 UT and peaked at 15:41 UT, with Hα maximum at 15:33 UT from NOAA active region 8933 at location N16W66. The Large Angle and Spectrometric Coronagraph (LASCO) on *SOHO* observed a halo CME with an asymmetric outline starting at 16:32 UT (hereafter CME 1) from the same active region with linear plane-of-sky velocity of 1188 km s^{-1}. The extrapolated CME-liftoff time is 14:47 UT ±5 minutes. The ≈45 MeV proton injection time (time at the Sun plus 8.3 minutes) calculated for the first, nonscattered particles

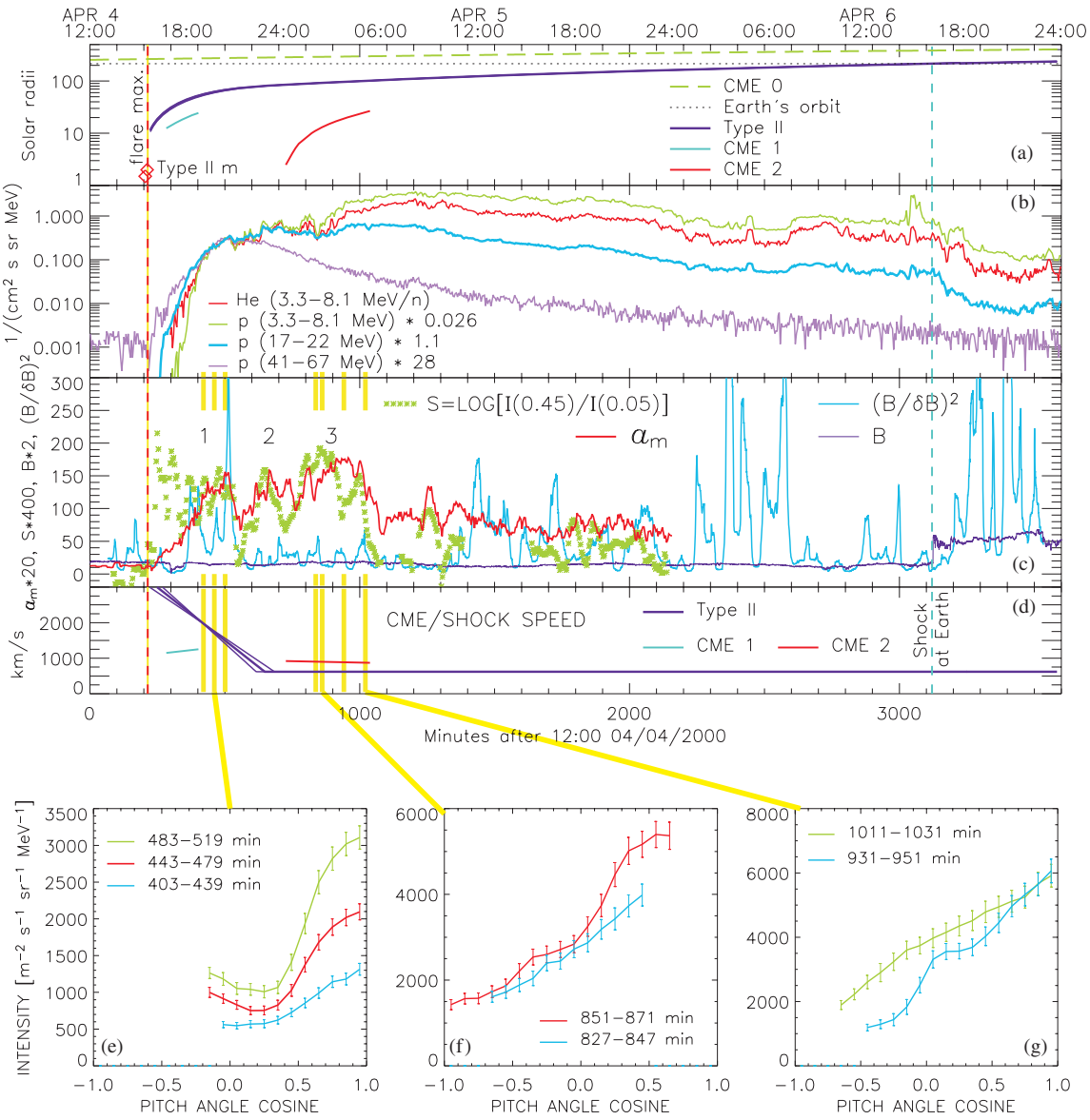

Figure 1. Overview of the 2000 April 4–6 event: (a) height–time profiles of associated CMEs/shocks; the CME speeds and heliocentric distances are the plane-of-sky coronagraph measurements, while the type II profile is a model fit to the dynamic radio spectrum; (b) re-normalized SEP intensity–time profiles; (c) the 17–22 MeV proton flux anisotropy index a_m and the gliding 36 minute average slope index S (both are defined in the text); along with the magnetic field intensity B and the reciprocal of the relative energy of magnetic fluctuations $1/(\delta B/B)^2$; (d) time–speed profiles of associated CMEs/shocks; (e–g) the 17–22 MeV proton pitch-angle distributions for a few selected time intervals.

traveling on a nominal path length of 1.2 AU was at 15:35 UT ±8 minutes, close to the flare maximum time. A similar timing also can be obtained with a velocity dispersion analysis. A metric type II radio burst, caused by a shock propagating in solar corona, seems to start at 15:25 UT and to continue for a few minutes, accompanied by a more prolonged type IV burst (15:15–16:19 UT). A decametric type II burst was seen by the *Wind*/WAVES receiver starting at about 15:40 UT, April 4. Two days later, on April 6, the interplanetary shock passage was observed near the Earth's orbit at 16:01, 16:04, and 16:27 UT by *SOHO*, *ACE*, and *Wind*, respectively.

Figure 1 illustrates different facets of the observed event. Panels (a) and (d) show the plane-of-sky CME distances and speeds deduced from the LASCO observations and the three-dimensional radial distance and speed of the interplanetary shock inferred from the radio type II burst observations by *Wind*/WAVES. The SEP intensity–time profiles observed with *SOHO*/ERNE are shown in panel (b), while the SEP anisotropy indexes (ERNE/HED) and the magnetic field parameters (*ACE*/MAG) are in panel (c). All intensity–time profiles shown in Figure 1(b) have been normalized to the same intensity of the first peak, to reveal the changes in the helium-to-proton abundance ratio and in the proton energy spectrum before and after the peak. The high-precision proton pitch-angle distributions observed with ERNE/HED at the times indicated with vertical yellow lines are shown in panels (e)–(g). All the panels are described in detail below.

The low-frequency type II radio burst associated with CME 1 is shown in Figure 2. The type II burst was observable only at twofold plasma frequency (harmonic), which was the case also in a number of other events (e.g., Reiner et al. 2007). We are concerned here with the propagation of the shock through the interplanetary medium, where the plasma density is known to fall off approximately as $1/R^2$, which suggests that the shock

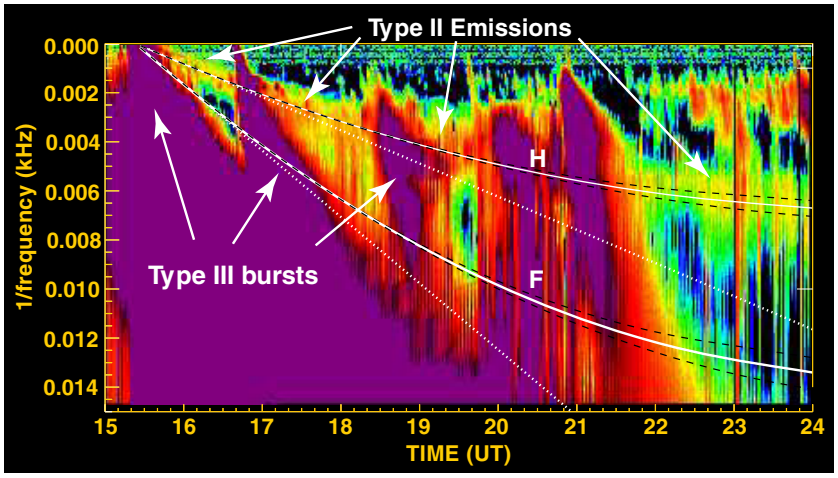

Figure 2. Dynamic spectrum from the *Wind*/WAVES experiment, plotted as inverse frequency vs. time, showing the decametric–kilometric type II radio emissions till the end of 2000 April 4. The curves show the data fits with the decelerating shock model (fundamental, F, and harmonic, H), while straight lines illustrate the expected dynamics of type II spectrum in the case of a constant speed shock.

deceleration may be rendered more obvious in the frequency drifting radio data if it is plotted as the inverse frequency versus time, rather than the traditional way of plotting frequency versus time, because $1/f \propto R(t)$. The radio data for the 2000 April 4 event are plotted in this way. The kinematic parameters of the interplanetary type II shock between $\sim 10 R_\odot$ and 1 AU can be estimated using the method described by Reiner et al. (2007). First, the shock speed at 1 AU was solved from the Rankine–Hugoniot equations, using the in situ plasma and field data, and found to be 620 km s^{-1}, which to an accuracy of 5% coincides with a simple estimate based on the differences between the shock arrival times at *SOHO*, *ACE*, and *Wind*. The value of the 1 AU shock speed, compared to the 1188 km s^{-1} plane-of-sky velocity of LASCO CME, already implies that CME 1 has decelerated significantly during its interplanetary transport. A radial speed profile of the CME-1 shock was then deduced from the constraints imposed by the shock speed at 1 AU, the total Sun–Earth transit time, and the type II burst spectrum observed by *Wind*/WAVES, based on the assumption that the CME initially decelerated at a constant rate and then propagated at a constant speed to 1 AU. In Figure 2, two straight lines (fundamental and harmonic) illustrate the expected dynamics of type II spectrum in the case of a constant speed shock in contrast to the curves deduced with the decelerating shock model for three values of the deceleration rate: $-a = 85.7, 99.5$ (best fit), and 114 m s^{-2}. The inferred kinematic parameters of the type II shock are shown in Figures 1(a) and (d).

While CME 1 was traveling in the interplanetary space toward the Earth, at 00:06 UT on April 5, another CME appeared on the southwest of the solar disc (hereafter CME 2), first seen at $2.48 R_\odot$ around 212° central position angle with width of 68° and linear plane-of-sky speed of 898 km s^{-1}. At that time, the inferred heliocentric distance of the type II shock of CME 1 was about 0.4 AU. Although there were no type II bursts associated with the new CME, a new intensity rise was observed in SEPs (Figure 1(b)). The old SEP event had masked the raising phase of the new particle event, so that a velocity dispersion in the second event can be found only in the maximum intensity time observed in the different energy channels. However, a new streaming of ~20 MeV protons was detected with ERNE/HED by the change in their pitch-angle distribution (Figure 1(f)), associated with changes also in the proton energy spectrum and in the He/p abundance ratio (those changes are evident from the separation between the corresponding intensity profiles in Figure 1(b)).

Panel (f) shows the rise of the new proton stream from the Sun along the interplanetary magnetic field, over the remnant flux of the previous event, while panel (e) shows the onset of the first event and panel (g) illustrates evolution of the pitch-angle distribution after the final rise phase. A remarkable feature in Figure 1(e) is the indication of the particle streaming not only from the Sun but also in the opposite direction (the distribution increase toward negative pitch-angle cosines, μ). This feature could be caused by the bouncing of protons at a magnetic mirror behind the Earth's orbit (to be discussed in detail in Section 3).

As overview of the proton flux anisotropy development, we plot in Figure 1(c) an empirical anisotropy index, a_m, and a pitch-angle distribution slope index, S. The anisotropy index is the difference between the 5 highest and the 30 lowest intensities in the ERNE/HED directional bins divided by an error calculated so that it takes into account both the uncertainty due to Poisson statistics and the error of averaging between the bins. The slope index, S, is the natural logarithm of the proton intensity ratio of the directions $\mu = 0.45$ and $\mu = 0.05$. The index S is indicative of particle streaming from the Sun, while the anisotropy index a_m can also reveal other types of anisotropic distributions, e.g., a loss-cone distribution. The indexes have been re-normalized to be comparable to each other at the first stages of the event (periods 1–3). In those periods, when the anisotropy is dominated by particle streaming from the Sun, S and a_m are well correlated. Separation of the curves S and a_m in the late phase of the event indicates that the anisotropy is not caused mainly by the streaming.

In Figure 1(c), we additionally compare the SEP anisotropy indexes with the inverse relative magnetic energy of the solar wind turbulence, $(B/\delta B)^2$, because the turbulence level is among the most important factors affecting the SEP flux anisotropy and one could expect a correlation between $(B/\delta B)^2$, on the one hand, and S (or a_m) on the other (Kocharov et al. 2007, Equation (5), Figure 5, and discussion therein). The magnitude δB corresponds here to the magnetic fluctuations in the resonant scale range, which has been approximated as 0.1–10 Larmor radii of 20 MeV proton. The anisotropy indexes have been

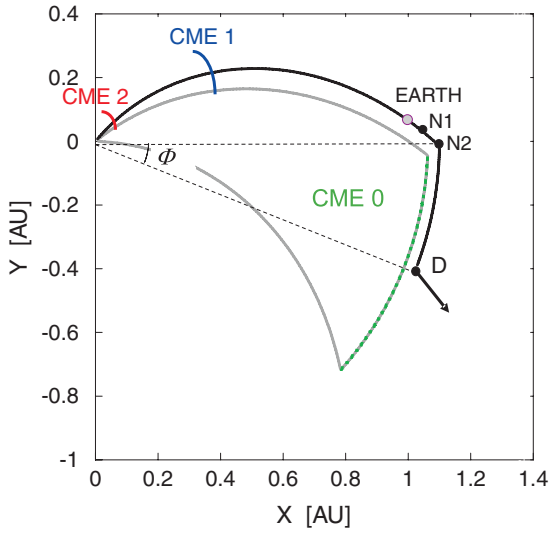

Figure 3. Model magnetic field structure with imaginary 1 AU spacecraft in the magnetic tube 0-N1-N2-D that is draped around the CME 0.

re-normalized to become comparable to $(B/\delta B)^2$ in period 1, but they turn out to be not correlated with $(B/\delta B)^2$ for the most part of the event.

3. DISCUSSION

The intensity–time profiles and elemental abundances during large SEP events typically show a complex variation with time (Klecker et al. 2006). The ERNE data reveal a fast evolution of He/p abundance ratio in the beginning of the 2000 April 4 event: the first rise of 3.3–8.1 MeV nucleon^{-1} He ions starts before the rise of protons of the same energy per nucleon and nearly simultaneously with rise of ≈4 times more energetic, 17–22 MeV protons (similar patterns were previously observed in some other events; Cohen et al. 2005; Mason et al. 2006). This helium-rich onset of the SEP event is followed by: (1) a period of constant energy spectrum and constant He/p abundance ratio, (2) the proton energy spectrum softening at >20 MeV with unchanged spectrum below 20 MeV and unchanged He/p, and then (3) a period of the new, softer energy spectrum in the entire energy range and the new He/p abundance ratio. There are corresponding enhancements in the SEP flux anisotropy in each period (Figure 1(c)).

A comparison of the SEP anisotropy indexes a_m and S with the magnetic fluctuation profile $(B/\delta B)^2$ reveals no overall correlation, which suggests that a variation of scattering frequency was not the main factor shaping the SEP anisotropy in the 2000 April 4 event. The 17–22 MeV proton distribution slope S (Figure 1(c)) indicates the particle streaming from the Sun and hence the SEP production at the source during the periods 1 and 2, as well as in the initial part of the period 3. The first period of the SEP production starts with the flare and CME-liftoff (CME 1) and with the metric type II shock in solar corona, then continues during the high-speed phase of the interplanetary type II shock observed by *Wind*/WAVES (Figure 1(d)). A straightforward explanation of the first period is particle acceleration by coronal shocks followed by (re-)acceleration at the interplanetary shock within ≈0.3 AU from the Sun.

Period 3 is associated with a new solar eruption (CME 2). At that time, the shock driven by CME 1 is between the Sun and the Earth, and surprisingly is not an obstacle for the fresh

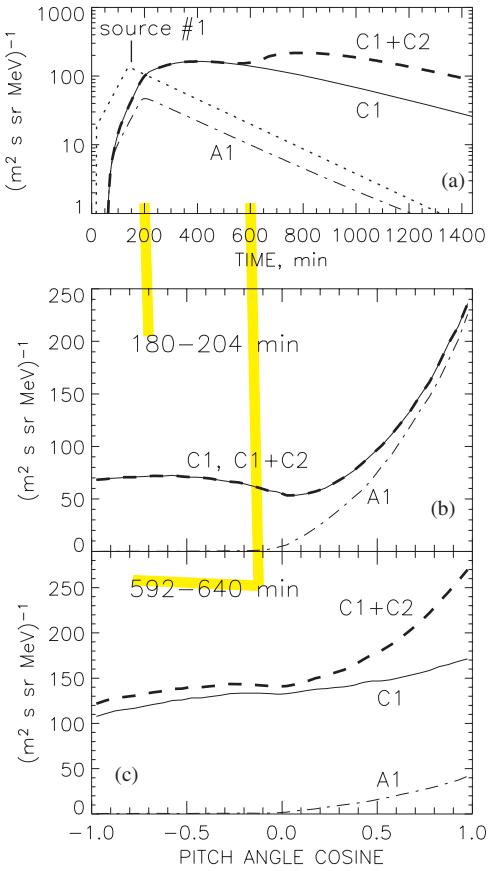

Figure 4. (a) Model time profile of the first SEP source at the Sun (source No. 1; arbitrary units; shifted by +8 minutes) and simulated intensity–time profiles of 17–22 MeV protons as observed at the Earth's orbit (A1, C1, and C1+C2; different curves are explained in the text). (b, c) The corresponding pitch-angle distributions for the two selected time intervals.

solar protons to directly access 1 AU. Arrival of the new proton beam along the interplanetary magnetic field line is clearly seen in Figure 1(f). The inferred speed profile of the interplanetary type II shock (Figure 1(d)) suggests that the shock of CME 1 had decelerated and weakened before the new SEPs were produced behind it by CME 2. The SEP data imply that the near-shock turbulence had also weakened and the freshly accelerated solar protons were able to penetrate through the shock of CME 1 without strong scattering, which in its turn implies that the CME-1 shock could not be an efficient ion accelerator by that time. We also speculate that the SEP production of period 2 could be caused by the escape of particles previously accelerated at the CME-1 shock and confined in its downstream region until the shock has weakened. However, most of the >40 MeV protons seem to be released before the period 2. The main SEP production due to the two successive eruptions together continues at ∼20 MeV for ∼12 hr.

The ERNE/HED directional measurements show a feature in the beginning of the 2000 April 4 event (Figure 1(e)) that can be related to the solar particles bouncing back at a bottleneck structure induced by an old interplanetary CME behind the Earth's orbit. On March 31, a partial halo CME was observed at the Sun by LASCO/C2 at 07:31 UT; with kinetic energy 8×10^{30} erg and angular width 101°; associated with a flare at 55° east. The linear speed measured by LASCO for that CME (hereafter CME 0) was 483 km s^{-1}, which could make it at ≈1.2 AU when the first SEPs were injected from the Sun on April 4 at ≈ 15:30 UT (Figure 1(a)). In addition, we note that at the

beginning of the day April 4, *ACE* at 0.99 AU observed the arrival of significant enhancement in the interplanetary magnetic field, which, however, was neither a magnetic cloud nor shock. For these reasons, we suggest that SEPs of the April 4 event were mirrored by the interplanetary magnetic field enhancement (draping) at the west flank of the interplanetary extension of CME 0.

As an estimate of the mirroring effect on SEPs, we have modeled two successive SEP events, No. 1 and No. 2, in a compressed interplanetary magnetic tube with a bottleneck situated behind the Earth's orbit, the tube 0–N1–N2–D in Figure 3. Implementation of the particle transport simulations is similar to that by Kocharov et al. (2007), but instead of a closed interplanetary magnetic loop we consider a structure that is open at the end point D. Thus, the system comprises a piece of Archimedean spiral 0–N1, an exponential magnetic mirror N1–N2 with the magnetic mirror ratio $B_{N2}/B_{N1} = 4$, and a round arch N2–D of the angular span $\Phi = 10^{\circ}$. The system expands uniformly with a radial velocity of 450 km s^{-1}. Heliocentric distances of points N1 and N2 at the beginning of SEP event No. 1 are 1.05 and 1.15 AU, respectively. Energetic protons are injected near the Sun with a power-law energy spectrum and with a source time profile shown for the first eruption with dotted line in Figure 4(a) (source No. 1). A similar time profile but shifted in respect to the first one by +8 hr is adopted also for source No. 2. The energy spectrum indexes are 4.5 and 6 for the sources No. 1 and No. 2, respectively. Each source, No. 1 or No. 2, is normalized to the time-integrated number of injected >15 MeV protons being 2×10^{30} per sr of heliocentric solid angle at the solar wind base. Similar to Kocharov et al. (2007), the parallel mean free path for the SEP transport is presumed to change linearly with distance from the Sun between 0.1 AU and N2 and to stay constant in the rest of the magnetic flux tube. Based on the anisotropy observed around the first intensity peak, we adopt the normalization mean free path value of 3 AU for the 10 MeV protons at the Earth's orbit. The energy and angular dependencies of the scattering frequency correspond to the Kolmogorov spectrum turbulence.

Figure 4(a) shows intensity–time profiles of 17–22 MeV protons for the model SEP event induced in the magnetic tube 0–N1–N2–D by source No. 1 (C1—solid line) and by two sources No. 1+No. 2 (C1+C2—dashed line), and in the standard solar wind only by source No. 1 (A1—dot-dashed line). Panels (b) and (c) show the corresponding pitch-angle distributions of 17–22 MeV protons for two selected time intervals indicated in the figure. The simulated intensity–time profile (Figure 4(a)) and pitch-angle distributions (Figures 4(b) and (c)) are qualitatively similar to those observed in the 2000 April 4 event (Figures 1(b), (e), and (f)), even if the simplified model does not fit exactly what is observed. The SEP event in the distorted solar wind is more intense and more prolonged than would be expected based on SEP simulations in the standard Archimedean spiral field (Figure 4(a), C1 versus A1).

We conclude that features of the 2000 April 4–6 event can be qualitatively explained by the SEP acceleration at the coronal and decelerating interplanetary shocks of the first CME and by the particles produced by the second CME behind the first one, being enhanced by the temporal confinement of energetic particles in a large-scale interplanetary magnetic trap. More modeling work is still required in order that the observed event be precisely fitted.

Accurate SEP anisotropy data are needed in each particular energy range to infer a scenario of the particles' acceleration and transport. The proposed particle telescope LET on *Solar Orbiter* will allow investigating the SEP energy range 1.5–20 MeV $nucleon^{-1}$ (Valtonen et al. 2007). In situ observations of decelerating shocks and SEPs on *Solar Orbiter*, with its orbit perihelion at 0.23 AU, could refine the scenario inferred here from the 1 AU data.

REFERENCES

Bougeret, J. L., et al. 1995, Space Sci. Rev., 71, 231
Cliver, E. W., Kahler, S. W., & Reames, D. V. 2004, ApJ, 605, 902
Cohen, C. M. S., et al. 2005, J. Geophys. Res., 110, A09S16
Gopalswamy, N. 2003, Geophys. Res. Lett., 30, 8013
Gopalswamy, N., et al. 2005, J. Geophys. Res. Space Phys., 110, A12S07
Klecker, B., et al. 2006, Space Sci. Rev., 123, 217
Kocharov, L., Saloniemi, O., Torsti, J., Kovaltsov, G., & Riihonen, E. 2007, ApJ, 654, 1121
Marqué, C., Posner, A., & Klein, K.-L. 2006, ApJ, 642, 1222
Mason, G. M., et al. 2006, ApJ, 647, L65
Neal, J. S., Nichols, T. F., & Townsend, L. W. 2008, Space Weather, 6, S09004
Reames, D. V. 1999, Space Sci. Rev., 90, 413
Reiner, M. J., Kaiser, M. L., & Bougeret, J.-L. 2007, ApJ, 663, 1369
Torsti, J., Riihonen, E., & Kocharov, L. 2004, ApJ, 600, L83
Torsti, J., et al. 1995, Sol. Phys., 162, 505
Valtonen, E., et al. 2007, in Second Solar Orbiter Workshop, ed. E. Marsch (ESA SP-641; Noordwijk: ESA) (CD-ROM)